BMC Plant Biology

RESEARCH Open Access

Integrative transcriptome and metabolome analysis reveals candidate genes related to terpene synthesis in *Chrysanthemum* × *morifolium*

Kexin Yu[1], Yueheng Hu[1], Jingxuan Ye[1], Rui Ni[1], Runqiang Yang[2], Fadi Chen[1] and Aiping Song[1*]

Abstract

Background Chrysanthemum (*Chrysanthemum* × *morifolium*) is one of the four major cut flowers worldwide and is valued for ornamental, culinary, and medicinal purposes. Terpenoids are key components of the fragrance of chrysanthemum; they not only serve to repel insect herbivores and promote pollination but also impact the value of the plant. However, the terpene production of chrysanthemum and the regulatory mechanisms involved remain unclear.

Results We used gas chromatography–mass spectrometry (GC–MS) to identify 177 compounds, including 106 terpenes, in ten chrysanthemum cultivars. Monoterpene derivatives and sesquiterpenes were the most common. Next, we identified 27 candidate hub genes for terpene production in chrysanthemum via combined transcriptome and metabolome analysis, as well as weighted gene coexpression network analysis. The three terpenes synthesis-related genes were significantly expressed in the disc florets of the different chrysanthemum cultivars. We concluded that the transcription factors TCP8, TCP5, ATHB8, ATHB7, HAT22, TGA1, TGA4, and WHY1 may regulate terpene synthesis.

Conclusions In this study, we profiled terpenes in chrysanthemum florets and constructed a key terpene-transcription factor network related to terpene synthesis. These findings lay the groundwork for future research into the mechanism of terpene synthesis in chrysanthemum as well as in other plants.

Keywords Chrysanthemum, Terpenes, Transcriptome, Metabolome, Metabolome analysis

*Correspondence:
Aiping Song
aiping_song@njau.edu.cn
[1]State Key Laboratory of Crop Genetics and Germplasm Enhancement, Key Laboratory of Landscaping, Ministry of Agriculture and Rural Affairs, Key Laboratory of Biology of Ornamental Plants in East China, College of Horticulture, National Forestry and Grassland Administration, Sanya Institute of Nanjing Agricultural University, Nanjing Agricultural University, Nanjing 210095, China
[2]College of Food Science and Technology, Nanjing Agricultural University, Nanjing 210095, China

Background

Chrysanthemum (*Chrysanthemum* × *morifolium*) is a perennial flowering plant of the genus *Chrysanthemum* in the Asteraceae family (also known as Compositae) [1]. It is one of the top ten traditional flowers in China and one of the four major types of cut flowers in the world, with a wide range of ornamental, culinary, economic, and medicinal uses. Chrysanthemum has rich genetic resources and can be classified as tea chrysanthemum, medicinal chrysanthemum, or ornamental chrysanthemum based on the particular uses of the plant. Studies have shown that chrysanthemum tea not only can promote blood circulation and lower blood cholesterol levels but also has anti-inflammatory, antioxidant, and anticarcinogenic effects [2]. Its efficacy is dependent on the effective components—primarily chlorogenic acid, cynaroside, and so forth—contained in the chrysanthemum capitulum [3]. As market demand continues to rise annually, volatile compounds have become crucial indicators of the quality of chrysanthemum tea, significantly influencing its aroma and flavour [4]. Research indicates that most volatile compounds in tea chrysanthemums are composed of terpenoids, which play a pivotal role in defining the sensory characteristics of the tea, but the chrysanthemum terpenoid regulatory mechanism is still unclear, limiting the effectiveness of breeding chrysanthemum for enhanced terpenoid production.

The chrysanthemum capitulum is typically composed of an outer whorl of ray florets (bilateral symmetry) and an inner whorl of disc florets (radial symmetry) [5] and is rich in flower colour, diverse in flower type, and of high ornamental value. Chrysanthemum is well received by consumers, and cut chrysanthemums account for 30% of the total cut flowers worldwide; thus, it is an important component of the floral industry [6]. However, as the market demand for unique flower fragrances, types, and colours has increased, the breeding of high-quality chrysanthemum cultivars has remained limited. Therefore, developing new cut flower cultivars that are insect- and disease-resistant and that have superior flower colours and unique fragrances has become one of the most important goals of chrysanthemum breeding [7].

Terpenoids are the most abundant plant secondary metabolites and are frequently employed in the cosmetic and perfume industries. More than 60,000 terpenoid metabolites have been discovered, with more than 25,000 in plants [8, 9]. Terpenoids also play crucial roles in plant growth and development, as well as in enticing insects to pollinate and in resisting various stresses [10]. Furthermore, plants can produce certain terpenes in gaseous form, which is one of the primary factors in their floral and fruity fragrances. The terpene synthesis pathway is usually divided into three stages. The first stage involves the generation of the C5 precursors isopentenyl diphosphate (IPP) and dimethyl diphosphate (DMAPP), during which the synthesis of terpenes can be divided into two pathways: the mevalonate (MVA) pathway [11] and the methylerythritol phosphate (MEP) pathway [12]. The second phase involves the biosynthesis of various terpenoid precursors, such as farnesyl pyrophosphate (FPP), which serves as a direct precursor for sesquiterpenes and triterpenes; geranylgeranyl pyrophosphate (GGPP), the direct precursor for diterpenes; and geranyl pyrophosphate (GPP), the precursor for monoterpenes. This stage is critical for establishing the foundational compounds necessary to produce diverse terpenoid classes. The third phase involves terpene generation and modification (redox, acylation, glycosylation, etc.), which determines the diversity of terpene compound structures [13].

To date, at least six TF families (AP2/ERF, bHLH, MYB, NAC, WRKY, and bZIP) related to terpenoid metabolism have been identified in plants [14]. For example, in *Artemisia caruifolia*, transcription factors from the AP2 family, AaERF1 and AaERF2, can bind to the *CRTDREHVCBF2 (CBF2)* and *RAV1AAT (RAA)* motifs found in the *ADS* and *CYP71AV1* gene promoters, stimulating their expression and contributing to artemisinin production [15]. In rice (*Oryza sativa*), the bHLH transcription factor DPF promotes the synthesis of diterpenoid phytoalexins (DPs) by activating the promoters of *COPALYL DIPHOSPHATE SYNTHASE2 (CPS2)* and *CYTOCHROME P450 monooxygenase 99A2* (*CYP99A2*) [16]. In the MYB transcription factor family, BpMYB21 increases the synthesis of triterpenoid chemicals in birch (*Betula platyphylla*), whereas BpMYB61 inhibits triterpenoid production [17]. Transcription factors control the transcription of plant genes not only independently but also in complexes that coregulate gene transcription. In Madagascar periwinkle (*Catharanthus roseus*), CrWRKY1 interacts with ORCA2/3, CrMYC2, and ZCTs to downregulate the expression of the latter three genes, reducing monoterpene synthase activity and thereby controlling monoterpene synthesis [18].

Studies have shown that terpenoids are the primary volatile components and metabolic products in chrysanthemum [19, 20]. These genes not only contribute significantly to the floral fragrance, influencing the scent quality of chrysanthemum, but they also play crucial roles in the stress response and signal transduction. Additionally, some terpenoids possess medicinal properties. Previous research has shown that chrysanthemum floral extract components are primarily monoterpenes, sesquiterpenes, and oxygenated monoterpenes [21], but the mechanism of terpene biosynthesis regulation in chrysanthemum remains unclear. In this study, ten chrysanthemum cultivars were used as research subjects, and joint transcriptome and metabolome analyses were performed to identify candidate genes involved in the

regulation of terpene biosynthesis and hub genes related to terpenoids. These findings provide a foundational framework for the terpene biosynthesis regulatory network, facilitating a deeper exploration of terpene-associated genes to define breeding targets and expand market applications.

Materials and methods

Experimental site and plant materials

Ten chrysanthemum cultivars used in this study were collected from the Chrysanthemum Germplasm Resource Preserving Centre (Nanjing Agricultural University, Nanjing, Jiangsu, China). The plants were cultivated under identical greenhouse conditions and natural light until they reached the half-blooming stage, with sampling conducted approximately 60 days after planting. Tissue samples of 0.2 g from ray and disc florets were collected from each cultivar (except from 'Carice'disc florets), with 3 individual replicates, resulting in a total of 57 samples (Fig. 1) that were designed as follows: ("G" indicates disc florets and "S" indicates ray florets).AG, 'Nannongxiangyang' disc florets; AS, 'Nannongxiangyang' ray florets; BG, 'Nannongwufengche' disc florets; BS, 'Nannongwufengche' ray florets; CG, 'Hangbaiju' disc florets; CS, 'Hangbaiju' ray florets; DG, 'Jinba' disc florets; DS, 'Jinba' ray florets; EG, 'Chuju' disc florets; ES, 'Chuju' ray florets; FG, 'Chihuang' disc florets; FS, 'Chihuang' ray florets; GG, 'Huangxiangli' disc florets; GS, 'Huangxiangli' ray florets; HG, 'Nannongqiaofengche' disc florets; HS, 'Nannongqiaofengche' ray florets; IS, 'Caliche' ray florets; JG, 'Nannongxiaolicui' disc florets; and JS, 'Nannongxiaolicui' ray florets. The same method was used to collect metabolomic samples.

GC–MS

To prepare for analysis, 0.2 g of each sample was ground to powder in liquid nitrogen and added to 1 ml of ethyl acetate solution containing 0.003% nonyl acetate. The mixture was then incubated for 2 h at room temperature (25 °C) with shaking and centrifuged at 4000 rpm for 5 min, after which 200 µl of the sample was loaded. The samples were analysed via triple quadrupole GC–MS (Agilent, California, USA) under the following conditions [22]. The extracts were separated on an HP-5 MS capillary column (30 m×0.25 mm×0.25 mm, Agilent Technologies Inc., Santa Rosa, CA, USA) with helium (99.999%) as the carrier gas at a flow rate of 1 mL/min. The initial temperature of the column was 50 °C, the temperature was increased to 180 °C at a rate of 5 °C/min and then increased to 270 °C at a rate of 20 °C/min, and the temperature was maintained at 270 °C for 5 min [19]. The MS conditions were as follows: EI ion source temperature, 230 °C; ionization energy, 70 eV; and mass scan range, 40–500 amu [23]. The qualitative analysis of the substances was based on comparisons with the National Institute of Standards and Technology (NIST). Each component was quantified according to its peak area versus the peak area of the internal standard (nonyl acetate), and the concentration was expressed as µg/g fresh weight. Wilcoxon test was used to confirm the significant differences of each compound in different floral types at a level of $P < 0.05$.

RNA extraction and transcriptome sequencing

Disc and ray florets from various chrysanthemum cultivars were chosen for RNA extraction using an RNA extraction kit (Huayueyang, China). The total RNA content was subsequently evaluated with a Nanodrop One Ultra-Micro Spectrophotometer (Thermo Fisher, USA), and RNA quality was verified using agarose gel electrophoresis.

The samples were subsequently sent to Annoroad Gene Technology (Beijing) for paired-end library sequencing using the BGISEQ sequencing platform, with circular

Fig. 1 Morphology of the capitula of ten chrysanthemum cultivars. On the left side of the figure are the complete flowers of various cultivars; on the upper right is the ray floret; and on the lower right is the disc floret. (**A**) 'Nannongxiangyang'. (**B**) 'Nannongwufengche'. (**C**) 'Hangbaiju'. (**D**) 'Jinba'. (**E**) 'Chuju'. (**F**) 'Chihuang'. (**G**) 'Huangxiangli'. (**H**) 'Nannongqiaofengche'. (**I**) 'Carice'. (**J**) 'Nannongxiaolicui'; scale bar = 1 cm

DNA libraries constructed based on the principles of DNA nanoball sequencing. Raw data (raw reads) in fastq format were initially processed using Trimmomatic (v0.39) [24] with the following parameters: ILLUMINACLIP: adapters.fa:2:30:10, LEADING:3, TRAILING:3, SLIDINGWINDOW:4:20, and MINLEN:36. During this step, clean data (clean reads) were obtained by removing reads containing adapters, reads with poly-N sequences, and low-quality reads. In addition, the Q20, Q30, and GC contents of the clean data were calculated. All downstream analyses were based on these high-quality clean data.

Weighted correlation network analysis (WGCNA)

HISAT2 (https://daehwankimlab.github.io/hisat2/) [25] was used to map the fastq files to the chrysanthemum reference genome [26], which was then quantified with featureCounts (v 2.0.0) (https://subread.sourceforge.net/) [27] to provide a matrix of count raw values. We used rnanorm (v 1.5.1) [28] to perform this conversion. The "-annotation" parameter was applied with a GTF file from the chrysanthemum genome, and the "--fpkm-output" parameter was used to output fragments per kilobase of exon per million fragments mapped (FPKM) values, which can be used to estimate the gene expression values of ray and disc floret RNAs in various chrysanthemum cultivars.

The FPKM value expression dataset was logarithmically transformed using the log2 (x + 1) algorithm. The "Mad" function in R was used to analyse the data. We sorted genes based on the degree of dispersion of their expression levels across all samples, from high to low, and selected the top 30% of genes that were selected for further analysis. Hierarchical clustering of the normalized transcript data was performed using the "hclust" function in R. Outliers were identified and excluded based on the clustering results. These expression patterns of genes were subsequently analysed using WGCNA [29], reshape2 [30], and stringr [31]. The soft threshold for the coexpression network was determined using the "pickSoftThreshold" function in the WGCNA package, and the soft threshold was set to 8. The network type was set to "unsigned", the minimum number of genes in a module was 30, and the merge threshold for merging "CutHeight" was 0.4. Modules with dissimilarity coefficients less than 0.4 were merged, and all the gene modules were generated. The "cor" function was used to calculate the correlation coefficient between gene modules and samples, the "corPvalueStudent" function was used to calculate the significance of the correlation, the data type was considered continuous, and the "labeledHeatmap" function was used to generate the correlation heatmap between modules and samples. The mRNAs in the modules were annotated with Gene Ontology (GO) and Kyoto Encyclopedia of Genes and Genomes (KEGG) [32], and the coding genes were analysed for functional enrichment. A heatmap was generated via https://www.bioinformatics.com.cn, an online platform for data analysis and visualization. Finally, relevant modules were chosen for visualization using Cytoscape software [33].

The final set of genes was first searched against the Chrysanthemum Genome Database (http://210.22.121.250:8880/asteraceae/homePage) to obtain their protein sequences. Subsequently, BLASTp analysis was performed on the TAIR website (https://www.arabidopsis.org/) using Arabidopsis as the reference.

Screening of transcription factors

We used ITAK (the Plant Transcription factor and Protein Kinase Identifier and Classifier) [34] to generate a list of predicted TFs in chrysanthemum, which we then compared against our set of 9,807 genes.

Visualization of hub genes

After sorting by edge weight, the genes in the five candidate modules were imported into Cytoscape. Using the cytoHubba plugin in Cytoscape with the maximal clique centrality (MCC) algorithm, nodes within the network are ranked on the basis of their properties. As a topological analysis method, the MCC evaluates the relationships between nodes and edges, demonstrating high accuracy in identifying hub genes. Upon completion, the result list displays nodes with increasingly intense colours representing higher scores and greater significance, indicating more critical genes. This analysis ultimately provides a ranked list of genes within each module. The cytoHubba plugin was used, and the MCC algorithm was used to determine the ranking of each gene in each module.

Results

Metabolomic profiles

GC–MS analysis revealed 177 compounds across the disc and ray florets of 10 chrysanthemum cultivars, including 106 terpenes and their derivatives. Among these, 62 are sesquiterpenes and sesquiterpene derivatives, 37 are monoterpenes and monoterpene derivatives, and 6 are diterpenes and diterpene derivatives (Additional file 1: Table S1).

A bar chart (Fig. 2) was created on the basis of the content of disc and ray florets of each cultivar of chrysanthemum in Table S1 (Additional file 1). The quantification of the compounds identified in the floral organs (Fig. 2) revealed that the amounts of monoterpenes and diterpenes were substantially lower across all the cultivars than were the other compounds. Notably, the total content of each terpene was significantly higher in the FG than in the other samples (Fig. 2). Additionally, the total content of each terpene in ray florets was lower than that

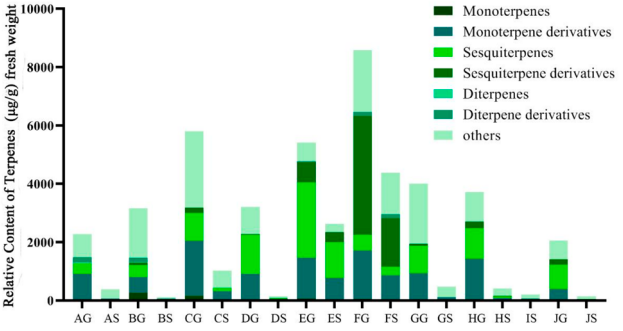

Fig. 2 Distribution of total terpene abundance of various terpene species in the disc and ray florets of 10 chrysanthemum varieties. (AG) 'Nannongxiangyang' disc florets. (AS) 'Nannongxiangyang' ray florets. (BG) 'Nannongwufengche' disc florets. (BS) 'Nannongwufengche' ray florets. (CG) 'Hangbaiju' disc florets. (CS) 'Hangbaiju' ray florets. (DG) 'Jinba' disc florets. (DS) 'Jinba' ray florets. (EG) 'Chuju' disc florets. (ES) 'Chuju' ray florets. (FG) 'Chihuang' disc florets. (FS) 'Chihuang' ray florets. (GG) 'Huangxiangli' disc florets. (GS) 'Huangxiangli' ray florets. (HG) 'Nannongqiaofengche' disc florets. (HS) 'Nannongqiaofengche' ray florets. (IS) 'Caliche' ray florets. (JG) 'Nannongxiaolicui' disc florets. (JS) 'Nannongxiaolicui' ray florets

in disc florets, suggesting that terpenes are more prevalent in disc florets (Fig. 2). Sesquiterpenes and monoterpene derivatives were particularly abundant across the various chrysanthemum cultivars (Fig. 2). Interestingly, compared with those of the other samples, the tea used chrysanthemums (EG, FG, CG) had the higher terpene contents (Fig. 2). Furthermore, the levels of sesquiterpene derivatives in FG and FS were higher than those in the other samples, as were the levels of sesquiterpenes in EG and ES (Fig. 2).

The total content of various terpenes in each cultivar was significantly higher in the disc floret group than in the ray floret group (Fig. 3). The results indicated that the terpene content is significantly higher in disc florets compared to ray florets for sesquiterpenes, sesquiterpene derivatives and monoterpene derivatives. Similarly, disc florets show a much higher monoterpenes content than ray florets.

RNA-seq analysis

In this study, 57 transcriptomes were sequenced, yielding 39,874,564 to 63,215,786 clean reads after adapters and low-quality sequences were removed, with sequencing data ranging from 5.57 G to 8.83 G per sample, for a total of 394.6 G of sequencing data (Table 1). The RNA-seq data were subsequently mapping to the chrysanthemum reference genome. Additionally, we performed a PCA of the average values of the RNA-seq data (Fig. 4). The tighter clustering of S in different cultivars suggests greater homogeneity compared to G, which shows a broader dispersion. In most cultivars, the expression patterns of disc florets are well distinguished from those of ray florets, but for F, the disc florets and ray florets samples presented more independent and distinct expression patterns.

Combined transcriptomic and metabolomic analysis

The top 30% of genes identified using the mad function were subjected to WGCNA and grouped into 39 coexpression modules (Additional file 5: Fig. S1A; Additional file 2: Table S2). The relationships between gene module expression and total terpenoid class abundances were assessed using correlation, with a Pearson correlation coefficient greater than 0.6 serving as a threshold (Fig. 5). These results revealed that modules that were significantly correlated with monoterpenes and diterpenes were absent; the turquoise module was significantly correlated with sesquiterpenes and monoterpene derivatives, with correlations of 0.70 and 0.69, respectively; and the brown module was strongly correlated with sesquiterpene derivatives and diterpene derivatives, with correlations of 0.60 and 0.75, respectively.

Modules and individual terpene levels were examined using correlation analysis (Additional file 5: Fig. S1B-H), and the terpenes found to be significantly correlated with the brown and turquoise modules were identified, with a Pearson correlation coefficient greater than 0.6 serving as the threshold value. On the basis of these results (Additional file 1: Table S1), DTD4 (neophytadiene) was significantly correlated with the brown module with a correlation of 0.64; MTD14 ((+)-2-Bornanone) was significantly correlated with the brown module with a correlation of 0.63; MTD2 (1,3-Cyclohexadiene-1-carboxaldehyde, 2,6,6-trimethyl-), MTD5 (2-Cyclohexen-1-one, 3-methyl-6-(1-methylethenyl)-, (S)-), MTD8 (2,6,6-Trimethylbicyclo[3.2.0]hept-2-en-7-one), MTD102 (Bicyclo[3.1.1]hept-3-en-2-one, 4,6,6-trimethyl-), and the turquoise module was significantly correlated, with correlations of 0.60, 0.63, 0.60, and 0.62, and STD14 ((S)-2,2,6-Trimethyl-6-((S)-4-methylcyclohex-3-en-1-yl)dihydro-2 H-pyran-3(4 H)-one), STD18 (.tau.-Muurolol), STD26 (2 H-Pyran-3-ol, tetrahydro-2,2,6-trimethyl-6-(4-methyl-3-cyclohexen-1-yl)-, [3 S-[3.alpha.,6.alpha.(R*)]]-), STD27 (2-Furanmethanol, tetrahydro-.alpha.,.alpha.,5- trimethyl-5-(4-methyl-3-cyclohexen-1-yl)-, [2 S-[2.alpha.,5.beta.(R*)]]-.) and brown were significantly correlated, with correlations of 0.61, 0.63, 0.64, and 0.60; ST29 (Tricyclo[5.4.0.0(2,8)] undec-9-ene, 2,6,6,9-tetramethyl-, (1R,2 S,7R,8R)-) was significantly correlated with the brown module, with a correlation of 0.65; and ST8 (Bicyclo[3.1.1]hept-2-ene, 2,6-dimethyl-6-(4-methyl-3-pentenyl)-), ST18 (1 H-Benzocycloheptene, 2,4a,5,6,7,8,9,9a-octahydro-3,5,5-trimethyl-9-methylene-, (4aS-cis)-) and ST28 (1 H-3a,7-Methanoazulene, 2,3,6,7,8,8a-hexahydro-1,4,9,9-tetramethyl-, (1α,3aα,7α,8aβ)-) and the turquoise

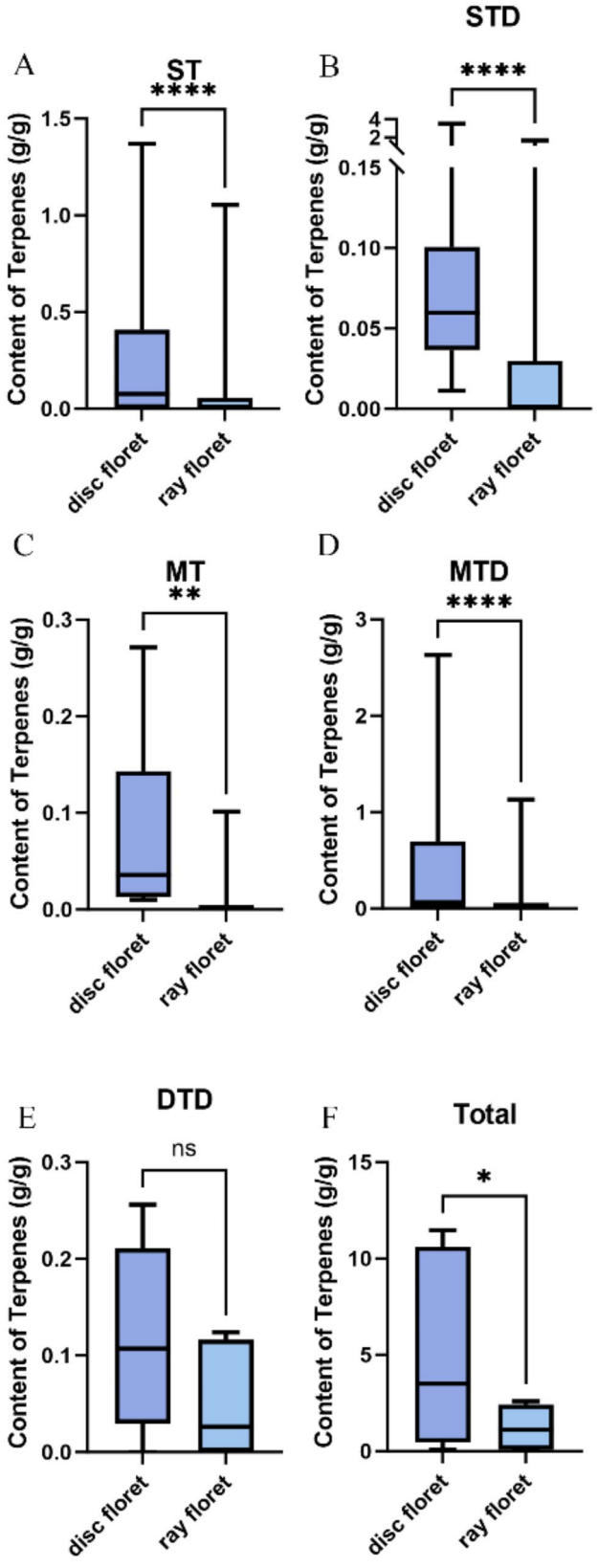

Fig. 3 The comparison of the differential contents of various terpenes in disc florets and ray florets. (**A**) Sesquiterpenes. (**B**) Sesquiterpene derivatives. (**C**) Monoterpenes. (**D**) Monoterpene derivatives. (**E**) Diterpene derivatives. (**F**) Total content of all terpenes

modules were significantly correlated, with correlation coefficients of 0.63, 0.70 and 0.80.

After preprocessing and network construction, we used the "exportNetworkToCytoscape" function to select genes on the basis of their correlation coefficients, with a threshold set at 0.02. These 9807 genes were identified from all the correlative modules considered in the analysis, representing a selection with a strong coexpression relationship from the total set of genes across all related modules. GO analysis revealed that biological processes (Fig. 6) were enriched primarily in "cellular metabolic processes" and "photosynthesis, light reaction". The cellular components were classified primarily as "thylakoid," "chloroplast envelope," and "ribosome".

Identification of transcription factors associated with terpenoid synthesis among the 9807 genes screened by WGCNA

Among the 9807 genes screened using WGCNA, 39 genes encoding transcription factors were identified (Additional file 3: Table S3), including 4 TCP, 11 bZIP, 6 HD-ZIP, 1 bHLH, 1 MADS, 2 whirly, 1 BES1/BZR1, 1 PLATZ, and 1 HSF family members. We visualized the genes associated with the TFs using Cytoscape (Additional file 5: Fig. S2). Among these family members, *TCP8* (*evm.TU.scaffold_48.95*, *evm.TU.scaffold_1008.400*), *ATHB8* (*evm.TU.scaffold_733.166*, *evm.TU.scaffold_1260.244*), *TGA1* (*evm.TU.scaffold_1692.129*), *TGA4* (*evm.TU.scaffold_1775.57*), *WHY1* (*evm.TU.scaffold_1817.231*), *HAT22* (*evm.TU.scaffold_1291.67*), *ATHB7* (*evm.TU.scaffold_1348.178*, *evm.TU.scaffold_8721.89*) and *bZIP5* (*evm.TU.scaffold_729.79*, *evm.TU.scaffold_9340.486*) have been reported to be associated with terpenoid synthesis from their orthologues from other plants [35–40].

Correlation module functional enrichment analysis

The KEGG functions were annotated based on the five modules (brown, cyan, green, pink, and turquoise) to which the screened transcription factor genes belonged. Although these modules themselves (cyan, green and pink) may not exhibit a significant correlation with terpenoid levels in our data, some of the transcription factors identified within these modules have been reported in the literature to be associated with terpenoid biosynthesis. Therefore, the presence of these transcription factors makes it valuable to explore their potential involvement in terpenoid synthesis. For visualization, the top 30 enriched KEGG pathways were selected. The results revealed that genes in the brown (Fig. 7A), turquoise (Fig. 7D), and green (Fig. 7C) modules were associated with the "metabolic pathway" and the "biosynthesis of secondary metabolites" pathway. Additionally,

Table 1 Information on RNA-seq

sample	library	raw_reads	clean_reads	clean_bases	error_rate	Q20	Q30	GC_pct	sample
AG_1	FRAS202435782-1r	48,124,880	46,571,114	6.99G	0.03	97.91	93.92	42.48	85.94%
AG_2	FRAS202435783-1r	55,657,798	54,219,936	8.13G	0.03	97.88	93.82	42.45	86.15%
AG_3	FRAS202435784-1r	46,703,970	45,419,366	6.81G	0.03	97.87	93.83	42.46	86.02%
AS_1	FRAS202435779-1r	48,222,800	46,816,240	7.02G	0.03	98.03	94.12	42.42	84.81%
AS_2	FRAS202435780-1r	55,577,662	53,905,676	8.09G	0.02	98.09	94.29	42.42	84.47%
AS_3	FRAS202435781-1r	57,829,512	56,528,328	8.48G	0.03	97.9	93.81	42.54	84.92%
BG_1	FRAS202435788-1r	48,090,686	46,925,718	7.04G	0.03	97.96	93.95	42.41	86.50%
BG_2	FRAS202435789-1r	50,391,120	49,092,658	7.36G	0.03	97.94	93.89	42.4	86.56%
BG_3	FRAS202435790-1r	51,852,824	50,395,454	7.56G	0.02	98.07	94.2	42.33	86.59%
BS_1	FRAS202435785-1r	52,972,804	51,605,170	7.74G	0.02	98.1	94.19	42.5	86.54%
BS_2	FRAS202435786-1r	51,978,244	50,417,374	7.56G	0.02	98.09	94.21	42.51	86.72%
BS_3	FRAS202435787-1r	47,399,488	46,342,714	6.95G	0.03	98	93.97	42.43	86.58%
CG_1	FRAS202435794-1r	52,182,284	50,621,214	7.59G	0.03	97.91	93.85	42.97	70.64%
CG_2	FRAS202435795-1r	58,252,326	56,179,026	8.43G	0.02	98.08	94.21	42.83	71.07%
CG_3	FRAS202435796-1r	58,497,138	56,525,956	8.48G	0.03	98	93.91	42.77	75.40%
CS_1	FRAS202435791-1r	44,651,698	43,460,514	6.52G	0.03	98.02	94.09	42.36	79.70%
CS_2	FRAS202435792-1r	56,826,278	55,267,720	8.29G	0.02	98.08	94.18	42.96	73.73%
CS_3	FRAS202435793-1r	56,755,060	55,035,236	8.26G	0.02	98.07	94.16	42.99	72.56%
DG_1	FRAS20H104437-1r	51,088,450	50,242,538	7.54G	0.03	97.56	92.9	42.14	86.18%
DG_2	FRAS202435801-1r	51,036,230	49,508,158	7.43G	0.03	97.91	93.92	42.45	86.68%
DG_3	FRAS202435802-1r	62,559,960	60,277,870	9.04G	0.03	97.98	94.06	42.63	86.84%
DS_1	FRAS202435797-1r	47,229,200	46,012,564	6.9G	0.03	98.02	94	42.29	85.86%
DS_2	FRAS202435798-1r	51,393,096	50,047,800	7.51G	0.02	98.06	94.17	42.4	86.15%
DS_3	FRAS202435799-1r	53,468,130	52,151,342	7.82G	0.03	98.04	94.13	42.78	86.48%
EG_1	FRAS202435806-1r	49,209,460	47,764,402	7.16G	0.03	97.96	93.94	42.18	84.53%
EG_2	FRAS202435807-1r	49,576,808	47,932,966	7.19G	0.03	97.97	93.97	42.17	85.19%
EG_3	FRAS202435808-1r	54,886,768	53,188,088	7.98G	0.03	97.98	93.94	41.97	84.86%
ES_1	FRAS202435803-1r	55,988,142	54,656,118	8.2G	0.03	97.95	93.87	42.2	84.58%
ES_2	FRAS202435804-1r	51,706,998	49,918,110	7.49G	0.02	98.08	94.17	42.02	84.62%
ES_3	FRAS202435805-1r	66,268,566	63,215,786	9.48G	0.02	98.11	94.27	42.94	85.63%
FG_1	FRAS202435812-1r	44,770,238	42,674,240	6.4G	0.03	97.63	92.57	42.55	80.35%
FG_2	FRAS202435813-1r	44,071,396	41,804,274	6.27G	0.03	97.55	92.51	42.54	81.43%
FG_3	FRAS202435814-1r	54,171,988	52,787,454	7.92G	0.03	98.04	94.08	42.86	81.74%
FS_1	FRAS202435809-1r	49,982,714	48,794,198	7.32G	0.02	98.28	94.6	42.54	75.99%
FS_2	FRAS202435810-1r	47,495,658	46,115,668	6.92G	0.02	98.23	94.49	42.62	77.20%
FS_3	FRAS202435811-1r	49,102,418	47,340,838	7.1G	0.02	98.23	94.49	42.62	76.68%
GG_1	FRAS202435818-1r	52,192,406	50,746,898	7.61G	0.02	98.09	94.18	43.9	51.04%
GG_2	FRAS202435819-1r	58,905,136	57,293,058	8.59G	0.02	98.2	94.44	43.82	49.95%
GG_3	FRAS202435820-1r	53,371,816	52,039,840	7.81G	0.02	98.24	94.5	44.26	43.10%
GS_1	FRAS202435815-1r	47,314,088	46,313,910	6.95G	0.02	98.26	94.62	44.59	36.36%
GS_2	FRAS202435816-1r	54,685,028	53,455,910	8.02G	0.02	98.19	94.42	44.2	42.87%
GS_3	FRAS202435817-1r	55,826,258	54,454,654	8.17G	0.02	98.27	94.61	44.37	38.50%
HG_1	FRAS202435824-1r	52,011,902	49,208,212	7.38G	0.02	98.13	94.35	42.28	87.27%
HG_2	FRAS202435825-1r	42,028,988	39,874,564	5.98G	0.03	97.62	92.69	42.61	87.20%
HG_3	FRAS202435826-1r	47,341,526	45,607,896	6.84G	0.02	98.15	94.35	42.25	87.50%
HS_1	FRAS202435821-1r	50,593,844	49,102,786	7.37G	0.02	98.12	94.22	42.07	85.95%
HS_2	FRAS202435822-1r	50,817,450	49,387,268	7.41G	0.02	98.08	94.17	42.23	85.68%
HS_3	FRAS202435823-1r	49,903,148	47,915,994	7.19G	0.03	98.04	94.07	42.24	85.78%
IS_1	FRAS202435827-1r	44,420,438	43,398,966	6.51G	0.02	98.08	94.2	42.49	86.81%
IS_2	FRAS202435828-1r	50,609,264	49,124,792	7.37G	0.02	98.14	94.24	42.19	86.77%
IS_3	FRAS202435829-1r	43,730,178	42,627,508	6.39G	0.02	98.15	94.24	42.22	86.86%
JG_1	FRAS202435833-1r	47,523,910	46,034,766	6.91G	0.03	97.94	93.73	41.91	86.83%
JG_2	FRAS202435834-1r	50,234,616	48,701,300	7.31G	0.03	98.03	93.98	42.07	86.99%

Table 1 (continued)

sample	library	raw_reads	clean_reads	clean_bases	error_rate	Q20	Q30	GC_pct	sample
JG_3	FRAS202435835-1r	46,116,572	44,466,688	6.67G	0.03	98.07	94.06	42	86.95%
JS_1	FRAS202435830-1r	47,302,330	45,557,604	6.83G	0.02	98.17	94.28	42.02	85.63%
JS_2	FRAS202435831-1r	44,474,642	42,927,928	6.44G	0.02	98.1	94.13	42.15	85.84%
JS_3	FRAS202435832-1r	48,069,996	47,017,640	7.05G	0.03	97.95	93.77	42.12	85.98%

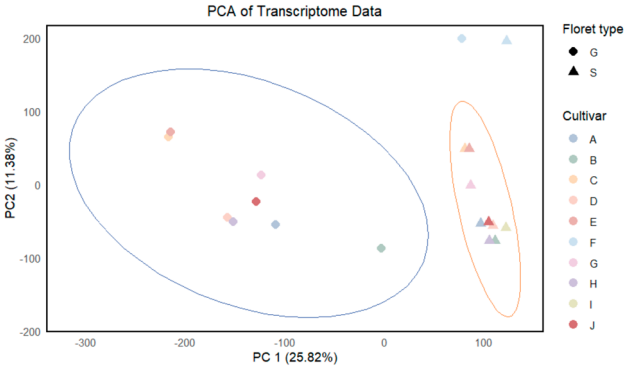

Fig. 4 PCA map of gene expression patterns of each sample. Cultivar: (A) 'Nannongxiangyang'. (B) 'Nannongwufengche'. (C) 'Hangbaiju'. (D) 'Jinba'. (E) 'Chuju'. (F) 'Chihuang'. (G) 'Huangxiangli'. (H) 'Nannongqiaofengche'. (I) 'Caliche'. (J) 'Nannongxiaolicui'. Floret type: (G) "disc floret". (S) "ray floret"

genes in the brown module were significantly enriched in the "cytochrome P450" pathway (drug metabolism-cytochrome P450), a widespread supergene family of oxygenases that catalyse various secondary metabolic reactions in plants, including terpenoid synthesis and metabolism [33, 41–43]. Furthermore, genes in the cyan module (Fig. 7B) were enriched primarily in the monoterpenoid biosynthesis and secondary metabolite biosynthesis pathways. Moreover, genes in the pink module (Fig. 7E) were enriched in the 2-oxocarboxylic acid metabolism pathway, which also plays a role in terpenoid synthesis.

Genes associated with terpene synthesis

Six genes encoding terpene synthases were found among the 9807 genes screened after WGCNA. BLAST analysis revealed that the most relevant terpene synthesis genes in *A. thaliana* were *TPS* (*evm.TU.scaffold_277.39*), *TPS21* (*evm.TU.scaffold_841.79*), *TPS03* (*evm.TU.scaffold_1112.22*), *KS1* (*evm.TU.scaffold_1295.6*), *TPS14* (*evm.TU.scaffold_1489.202*), and *ABC33* (*evm.TU.scaffold_104.31*) (Additional file 4: Table S4). As shown in Fig. 8, the data were normalized, and the expression levels of six genes involved in terpene production were greater in disc flowers than in ray florets. Moreover, *TPS14* (*evm.TU.scaffold_1489.202*) presented the highest expression levels in JG. *ABC33* (*evm.TU.scaffold_104.31*) had elevated expression in EG. *TPS21* (*evm.TU.scaffold_841.79*) was significantly expressed in both CS and CG, with a higher level in CS than in CG. *KS1* (*evm.TU.scaffold_1295.6*) exhibited relatively high expression in AS. *TPS03* was highly expressed in the cultivar EG, which is used for tea. Additionally, significant expression levels of *TPS* were detected in FG. These findings suggest that the biosynthesis of terpenoid compounds by TPS, TPS03, TPS14, and ABC33 primarily occurs in disc florets, whereas the biosynthesis by TPS21 and KS1 mainly occurs in ray florets.

Candidate hub genes related to terpene synthesis

A total of 27 Hub genes (highly connected genes) were identified on the basis of the final scores of each gene (Table 2; Additional file 5: Fig. S3). Among these genes, *POX2*, *GDPD2*, and *CML3* within the turquoise module were further recognized as the most central and representative hub genes. This classification was determined by their significantly higher cytoHubba scores than those of the other genes, highlighting their pivotal role in terpene synthesis.

Discussion

In this study, using transcriptome analysis data, a coexpression network for disc and ray florets from various chrysanthemum cultivars was created, and 27 potential hub genes relevant to terpenoid production were identified. Previous studies revealed terpenoids in chrysanthemum are synthesized in stages across all organs and developmental processes [44–49]. However, previous studies focused on diploid wild *Chrysanthemum* species, making it challenging to obtain comprehensive information on hexaploid cultivated chrysanthemums. Furthermore, it also potentially limited the subsequent analysis, including the mining of key genes and important regulatory aspects. Recently, the elucidation of the genome of hexaploid cultivated chrysanthemum has been supplemented by the annotation of hub genes encoding genes involved in terpenoid synthesis [26]. In this study, for the first time, the relationships between genes and the synthesis of different terpenoids in cultivated hexaploid chrysanthemum were investigated using combined transcriptome and metabolome analyses.

Terpenes associated with modules

Among the monoterpenes, sesquiterpenes, and diterpenes, as well as their derivatives that were found to be significantly associated with the brown and turquoise modules, ST18 ((4aS,9aR)-3,5-trimethyl-9-methylidene-2,4a,6,7,8,9a-hexahydro-1 H-benzo[7]annulene) has been found in the fruit oil of fennel (*Pimpinella anisum*

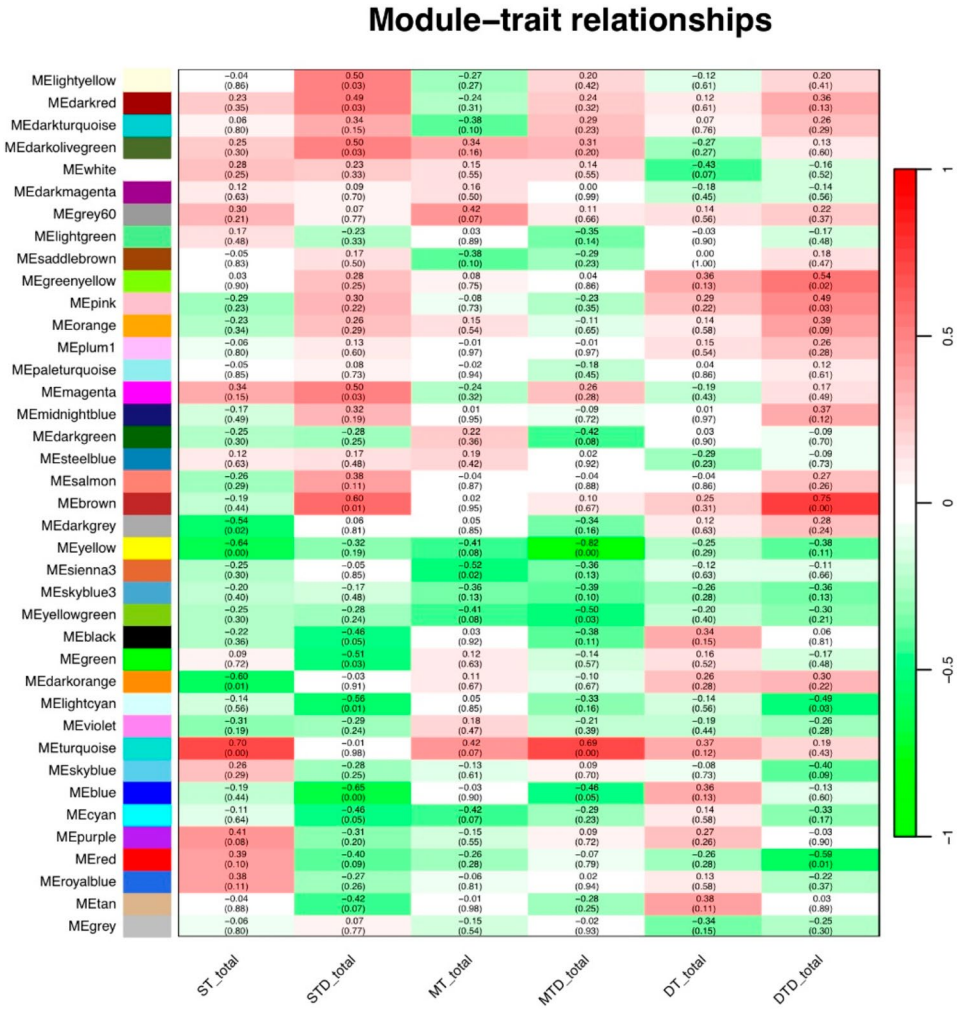

Fig. 5 Heatmap of correlations between expression modules and the total amount of various terpenoids. The y-axis coloured blocks represent modules associated with specific traits. On the x-axis: (ST_total): the total content of sesquiterpenes; (STD_total): the total content of sesquiterpene derivatives; (MT_total): the total content of monoterpenes; (MTD_total): the total content of monoterpene derivatives; (DT_total): the total content of diterpenes, (DTD_total): the total content of diterpene derivatives. This figure illustrates the relationships between various trait-associated modules and each type of compound

L.) at maturity and has bacteriostatic and highly valued olfactory properties [50]; STD14 ((S)-2,2,6-trimethyl-6-((S)-4-methylcyclohex-3-en-1-yl)dihydro-2 H- pyran-3(4 H)-one) is one of the main components of *Artemisia absinthium* essential oil (EO), which has high inhibitory activity against α-glucosidase and has the potential to treat diabetes mellitus [51]; STD26 (2 H-Pyran-3-ol) has antioxidant, antiapoptotic, and antimicrobial effects [52]; and DTD4, with the possible involvement of the GABAergic system, has anxiolytic-like and anticonvulsant activities [53]. These results are consistent with those for the candidate hub genes in the turquoise module (*POX2* (*evm.TU.scaffold_1786.55*), *GDPD2* (*evm.TU.scaffold_5019.9*, *evm.TU.scaffold_517.125*), *CML3* (*evm.TU.scaffold_1234.80*), *At1g54070* (*evm.TU.scaffold_339.74*), *WLIM2B* (*evm.TU.scaffold_2823.90*), and *KLCR2* (*evm.TU.scaffold_953.101*), *evm.TU.scaffold_1825.11*, *LFG4* (*evm.TU.scaffold_1089.142*), *At4g09580* (*evm.TU.scaffold_9043.147*)), which are significantly related to STD18 (.tau.-Muurolol) and are regarded as potential natural bactericides with antifungal activity for the control of fungal pathogens and are therefore valuable [47]. Additionally, MTD2 (1,3-cyclohexadiene-1-carboxaldehyde, 2,6,6-trimethyl-) acts as an anti-inflammatory agent and has antioxidant activity [54]; MTD10 (bicyclo [3.1.1] hept-3-en-2-one,4,6,6-trimethyl-) has in vivo and in vitro anti-inflammatory and anti-injury activities that confer anti-inflammatory and analgesic effects [55]. As a result, we speculated that the genes in the two modules function together in chrysanthemum to produce antibacterial and antioxidant effects. The screening of the hub genes in the modules, as well as further analysis of the possible genes, will benefit the breeding of new chrysanthemum

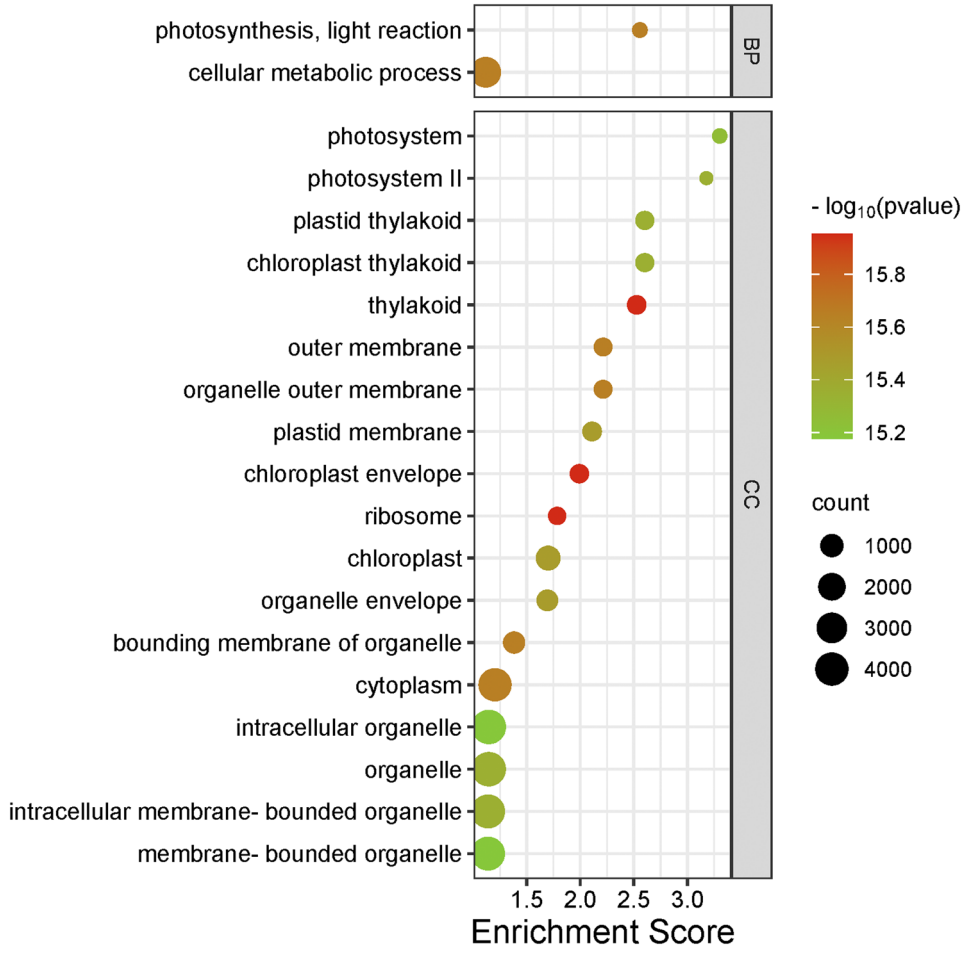

Fig. 6 GO enrichment map of 9807 genes. All genes are from the node list; "BP" refers to biological process, and "CC" refers to cellular component. In the legend, "count" refers to the number of genes that were annotated to each specific term in the GO analysis, whereas the "Enrichment score" represents the degree of enrichment of a particular GO term

cultivars with increased resistance to pests and diseases. The results of this study will also aid in achieving the cultivation goal of promoting chrysanthemum-related medicinal effects, such as anti-inflammatory effects, diabetes treatment, analgesic effects, and antianxiety effects.

Functional exploration of the relevant TPS

Plant terpenoids can be divided into primary and secondary metabolites on the basis of their functions. Terpenoids, such as gibberellin (GA), abscisic acid (ABA) and brassinolide (BR), as well as carotenoids and chlorophylls involved in plant photosynthesis, are among the primary metabolites. required for plant growth and development. Among the genes related to terpene synthesis, *ABC33* (*evm.TU.scaffold_104.31*) and *KS1* (*evm.TU.scaffold_277.39*) significantly affect gibberellin biosynthesis, resulting in plant growth and development [56]; *TPS* (*evm.TU.scaffold_277.39*), *TPS03* (*evm.TU.scaffold_1112.22*) and *TPS14* (*evm.TU.scaffold_1489.202*), on the other hand, affect the synthesis of monoterpene compounds in plants, with *TPS03* (*evm.TU.scaffold_1112.22*) mediating the attractiveness of plants to herbivorous insect predators and promoting insect pollination [57]. In *A. thaliana*, *TPS14* (*evm.TU.scaffold_1489.202*) catalyses the synthesis of linalool, thereby increasing plant resistance to aphids [55]. Furthermore, *TPS21* (*evm.TU.scaffold_841.79*) regulates the formation of (E)-β-stigmastigmine in *A. thaliana*, thereby regulating the biosynthesis of sesquiterpenes to influence the plant growth rate [58].

An integrative analysis was performed on the terpenoid profiles, the significance of terpenes in disc and ray florets, and the expression of TPSs in disc and ray florets across cultivars. It revealed that *TPS03* (*evm.TU.scaffold_1112.22*), *ABC33* (*evm.TU.scaffold_104.31*), *TPS14* (*evm.TU.scaffold_1489.202*) and *TPS* (*evm.TU.scaffold_277.39*) were highly expressed in the disc florets of each cultivar; *TPS21* (*evm.TU.scaffold_841.79*) and *KS1* (*evm.TU.scaffold_277.39*) were highly expressed in the ray florets of each cultivar. Monoterpene

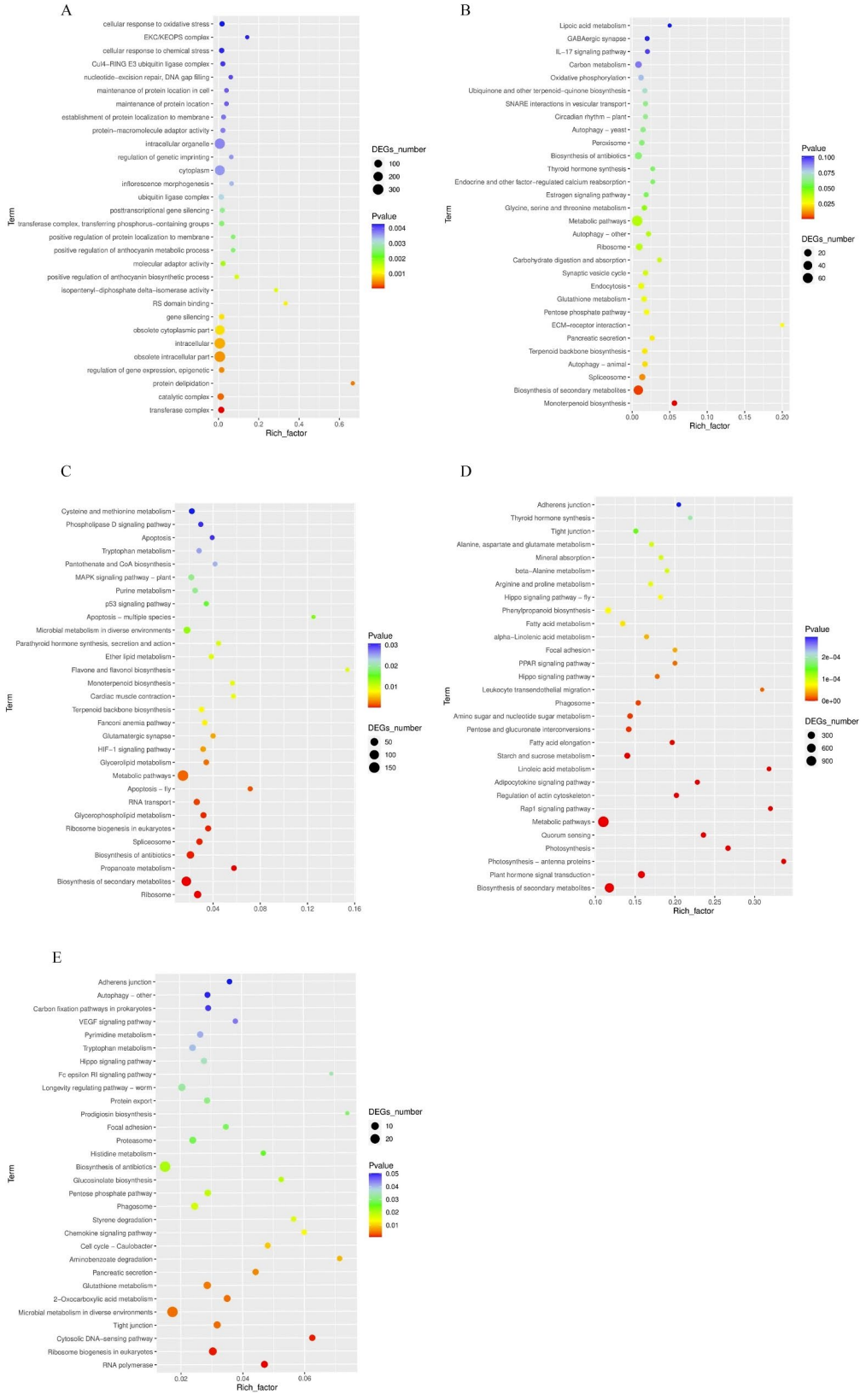

Fig. 7 KEGG enrichment plots of the modules. (**A**) Brown module. (**B**) Cyan module. (**C**) Green module. (**D**) Turquoise module. (**E**) Pink module. The "Rich_factor" indicates the degree of enrichment

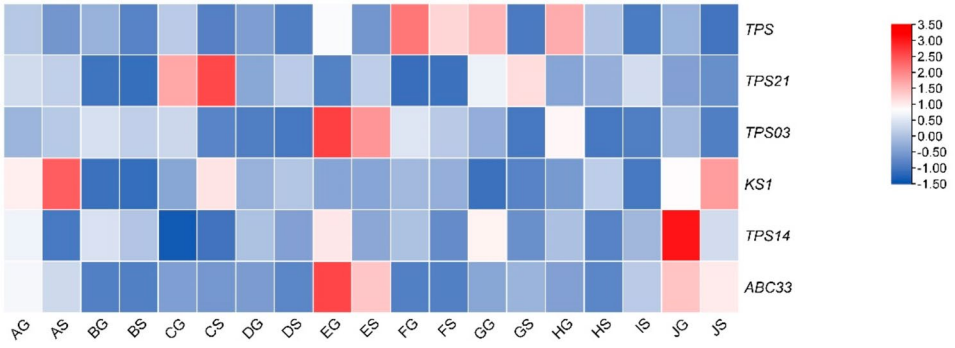

Fig. 8 Heatmap of the expression of six terpene synthases on the basis of FPKM values. (AG) 'Nannongxiangyang' disc florets. (AS) 'Nannongxiangyang' ray florets. (BG) 'Nannongwufengche' disc florets. (BS) 'Nannongwufengche' ray florets. (CG) 'Hangbaiju' disc florets. (CS) 'Hangbaiju' ray florets. (DG) 'Jinba' disc florets. (DS) 'Jinba' ray florets. (EG) 'Chuju' disc florets. (ES) 'Chuju' ray florets. (FG) 'Chihuang' disc florets. (FS) 'Chihuang' ray florets. (GG) 'Huangxiangli' disc florets. (GS) 'Huangxiangli' ray florets. (HG) 'Nannongqiaofengche' disc florets. (HS) 'Nannongqiaofengche' ray florets. (IS) 'Caliche' ray florets. (JG) 'Nannongxiaolicui' disc florets. (JS) 'Nannongxiaolicui' ray florets

Table 2 The total of Hubgene

Module	Gene Name
Brown	*SGT1*
	Mrpl47
	ChlADR1
	VHA-c"1
	DET2
	At5g12190
	SPL1
	RPS11
	CPA
	evm.TU.scaffold_96.144
Cyan	*evm.TU.scaffold_1358.45*
	HD2C
Turquoise	*POX2*
	KLCR2
	evm.TU.scaffold_1825.11
	LFG4
	CML3
	GDPD2
	At4g09580
	WLIM2B
	At1g54070
	GDPD2
Green	*RPL13B*
	evm.TU.scaffold_1769.90
	GPDP4
	evm.TU.scaffold_1266.81
Pink	*evm.TU.scaffold_1262.45*

derivatives and sesquiterpene substances were more highly expressed in the disc florets of the chrysanthemum plants. Given the previous studies [21], we propose that the terpenes within the disc florets play a key role in shaping their flavour and taste profile. Moreover, we performed a correlation analysis between the TPSs and all terpenoids (Additional file 1: Table S1; Additional file 5: Fig. S4). As a result, we found that *TPS03* (*evm.TU.scaffold_1112.22*), *ABC33* (*evm.TU.scaffold_104.31*), *TPS14* (*evm.TU.scaffold_1489.202*) and *TPS* (*evm.TU.scaffold_277.39*) mainly associated with the in the production of sesquiterpenes and sesquiterpene derivatives in disc florets; *TPS21* (*evm.TU.scaffold_841.79*) and *KS1* (*evm.TU.scaffold_277.39*) mainly associated the production of monoterpenes and monoterpene derivatives in ray florets. Furthermore, for the three tea used chrysanthemums (E, C, G), *TPS* (*evm.TU.scaffold_277.39*) were relatively high in GG, whereas *ABC33* (*evm.TU.scaffold_104.31*) and *TPS03* (*evm.TU.scaffold_1112.22*) were relatively high in EG. *TPS21* (*evm.TU.scaffold_841.79*) exhibited high expression levels in both CG and CS, with higher expression in CS than in CG. Moreover, the sesquiterpene content was much greater than that of other substances in EG, while the sesquiterpene and monoterpene derivative levels were more similar in GG. In CG, the substance content was much greater than that in CS, with the main substances being monoterpene derivatives and sesquiterpenes, and the content of monoterpene derivatives was greater than that of sesquiterpenes. Additionally, combining the above findings and the correlation analysis between TPS and all terpenoids, it was concluded that *ABC33* (*evm.TU.scaffold_104.31*)and *TPS03* (*evm.TU.scaffold_1112.22*) primarily regulate sesquiterpene synthesis in EG. *TPS* (*evm.TU.scaffold_277.39*) primarily regulated sesquiterpenes and monoterpene derivatives synthesis in GG. And *TPS21* (*evm.TU.scaffold_841.79*) may be involved in the regulation of monoterpene derivative synthesis and sesquiterpene synthesis in CS. According to the findings of previous studies, sesquiterpenes and monoterpenes are the primary components of chrysanthemum floral aroma [19]; therefore, *ABC33* (*evm.TU.scaffold_104.31*), *TPS03* (*evm.TU.scaffold_1112.22*), *TPS21* (*evm.TU.scaffold_841.79*) and *TPS* (*evm.TU.scaffold_277.39*) may be the key genes regulating

unique aroma generation in these three tea used chrysanthemum cultivars.

Core transcription factors

In addition, we discovered 39 core regulatory transcription factors organized into five modules. KEGG enrichment analysis revealed that the genes in these modules were highly enriched in two pathways: "metabolic pathway" and "secondary metabolite biosynthesis". Among the identified transcription factors, TCP8 directly binds and activates key BR synthesis genes [34], whereas *ATHB8* has also been linked to the differential expression of BR receptor-encoding genes in *Arabidopsis* [36]. Moreover, BR stimulates the salicylic acid (SA) response by inhibiting BIN2, which interacts with the transcription factors TGA1 and TGA4, enhancing plant immunity [37]. HAT22 has been shown to be necessary for ABA-mediated growth inhibition and leaf yellowing [38]. Water deprivation and ABA also increased *ATHB7* expression in *Arabidopsis* [39], whereas plastid-localized WHY1 improved the *Arabidopsis* seedling ABA response [40]. We therefore inferred that these transcription factors, which regulate the synthesis of terpenoids in chrysanthemum plants, may play various roles, such as mediating plant growth, leaf etiolation, and immunity to external factors.

Conclusion

In conclusion, through integrated transcriptomic and metabolomic analyses, this study identified 27 hub genes associated with the biosynthesis of terpenoid compounds. Additionally, six genes encoding terpenoid biosynthetic enzymes were found to influence plant growth and development by modulating primary and secondary metabolites, increasing pest resistance, and attracting insect pollinators. Furthermore, 39 transcription factor genes involved in the regulation of terpene metabolism were identified. These candidates merit additional functional validation through overexpression and gene knockout experiments to elucidate their specific roles, which offers valuable candidate genes and a comprehensive data resource for molecular biology research, supporting further exploration of terpenoid biosynthesis in chrysanthemum.

Supplementary Information

The online version contains supplementary material available at https://doi.org/10.1186/s12870-025-06163-z.

Supplementary Material 1: Fig. S1. Hierarchical Clustering and Module–Trait Relationships in Gene Co-Expression Analysis.

Supplementary Material 2: Fig. S2. Correlation network visualization of the TFs.

Supplementary Material 3: Fig. S3. Correlation network visualization of the hub genes.

Supplementary Material 4: Fig. S4. Heatmap of the correlation between TPSs and Terpenoids.

Supplementary Material 5: Table S1. Terpenoid collection.

Supplementary Material 6: Table S2. Correlative modules with their counts.

Supplementary Material 7: Table S3. Transcription factors encoded by relevant genes.

Supplementary Material 8: Table S4. Genes associated with terpene synthesis.

Acknowledgements

Not applicable.

Author contributions

K.Y. and Y.H. wrote the main manuscript text and R.N. and J.Y. prepared figures. A.S., R.Y. and F.C. reviewed the manuscript. All authors read and approved the final manuscript.

Funding

This research was funded by the Forestry Science and Technology Innovation and Promotion Project in Jiangsu Province (LYKJ[2023]22), the National Natural Science Foundation of China (32172609), the Achievement Transformation Fund project of Hainan Research Institute of Nanjing Agricultural University (NAUSY-CG-YB04), the "Blue Project" of Jiangsu Higher Education Institutions and a project funded by the Priority Academic Program Development of Jiangsu Higher Education Institutions.

Data availability

The transcriptome data has been uploaded to the National Center for Biotechnology Information with the accession number PRJNA1129914.

Declarations

Ethics approval and consent to participate

Our research did not involve any human or animal subjects, material, or data. The plant materials used in this study were obtained from the Life Science Building of Nanjing Agricultural University. We declare that the plant material in the experiment was collected and studied in accordance with relevant institutional, national, and international guidelines and legislation.

Consent for publication

Not applicable.

Competing interests

The authors declare no competing interests.

Received: 2 July 2024 / Accepted: 28 January 2025
Published online: 10 February 2025

References

1. Zhang W, Gao T, Li P, et al. Chrysanthemum Cm*WRKY53* negatively regulates the resistance of chrysanthemum to the aphid *Macrosiphoniella sanborni*[J]. Hortic Res. 2020;7(1):109.
2. Carullo G, Cappello AR, Frattaruolo L, et al. Quercetin and derivatives: useful tools in inflammation and pain management. Future Med Chem. 2017;9(1):79–93.
3. Kuang C-L, Lv D, Shen G-H, et al. Chemical composition and antimicrobial activities of volatile oil extracted from *Chrysanthemum morifolium* Ramat[J]. J Food Sci Technol. 2018;55(7):2786–94.
4. Ning X, Su J, Zhang X, et al. Evaluation of volatile compounds in tea chrysanthemum cultivars and elite hybrids. Sci Hort. 2023;320:112218.
5. Elomaa P, Zhao Y, Zhang T. Flower heads in Asteraceae—recruitment of conserved developmental regulators to control the flower-like inflorescence architecture[J]. Horticulture Research, Nature Publishing Group. 2018;5(1):1–10.

6. Anderson N. Flower Breeding and Genetics Issues, Challenges and Opportunities for the 21st Century: Issues, Challenges and Opportunities for the 21st Century[M]. 2006. https://doi.org/10.1007/1-4020-4428-3
7. Su J, Jiang J, Zhang F, et al. Current achievements and future prospects in the genetic breeding of chrysanthemum: a review[J]. Horticulture Research, Nature Publishing Group. 2019;6(1):1–19.
8. Brandt W, Bräuer L, Günnewich N, et al. Molecular and structural basis of metabolic diversity mediated by prenyldiphosphate converting enzymes[J]. Phytochemistry. 2009;70(15):1758–75.
9. Yonekura-Sakakibara K, Saito K. Functional genomics for plant natural product biosynthesis[J]. Nat Prod Rep. 2009;26(11):1466–87.
10. Gershenzon J, Dudareva N. The function of terpene natural products in the natural world[J]. Nat Chem Biology Nat Publishing Group. 2007;3(7):408–14.
11. Lange BM, Rujan T, Martin W, et al. Isoprenoid biosynthesis: the evolution of two ancient and distinct pathways across genomes[J]. Proceedings of the National Academy of Sciences, Proceedings of the National Academy of Sciences. 2000;97(24):13172–77.
12. Olofsson L, Engström A, Lundgren A, et al. Relative expression of genes of terpene metabolism in different tissues of *Artemisia annua* L.[J]. BMC Plant Biol. 2011;11(1):45.
13. Dudareva N, Klempien A, Muhlemann JK, Kaplan I. Biosynthesis, function and metabolic engineering of plant volatile organic compounds. New Phytol. 2013;198:16–32.
14. Xu Y, Zhu C, Xu C, et al. Integration of metabolite profiling and transcriptome analysis reveals genes related to volatile terpenoid metabolism in finger citron (C. *medica* var. *sarcodactylis*) [J]. Molecules, Multidisciplinary Digital Publishing Institute. 2019;24(14):2564.
15. Yu ZX, Li JX, Yang CQ, et al. The jasmonate-responsive AP2/ERF transcription factors AaERF1 and AaERF2 positively regulate artemisinin biosynthesis in *Artemisia annua* L.[J]. Molecular Plant, Elsevier. 2012;5(2):353–65.
16. Yamamura C, Mizutani E, Okada K, et al. Diterpenoid phytoalexin factor, a bHLH transcription factor, plays a central role in the biosynthesis of diterpenoid phytoalexins in rice[J]. Plant J. 2015;84(6):1100–13.
17. Yin J, Sun L, Li Y, et al. Functional identification of BpMYB21 and BpMYB61 transcription factors responding to MeJA and SA in Birch triterpenoid synthesis[J]. BMC Plant Biol. 2020;20(1):374.
18. Suttipanta N, Pattanaik S, Kulshrestha M, et al. The transcription factor CrWRKY1 positively regulates the terpenoid indole alkaloid biosynthesis in Catharanthus roseus[J]. Plant Physiol. 2011;157(4):2081–93.
19. Zhou Y, Abbas F, Wang Z, et al. HS–SPME–GC–MS and electronic nose reveal differences in the volatile profiles of Hedychium Flowers. Molecules. 2021;26(17):5425. https://doi.org/10.3390/molecules26175425
20. Yueheng H, Song A, Guan Z, et al. CmWRKY41 activates *CmHMGR2* and *CmFPPS2* to positively regulate sesquiterpenes synthesis in *Chrysanthemum morifolium*. Plant Physiol Biochem. 2023;196:821–9.
21. Sun H, Zhang T, Fan Q, et al. Identification of floral scent in chrysanthemum cultivars and wild relatives by gas chromatography-mass spectrometry[J]. Molecules, Multidisciplinary Digital Publishing Institute. 2015;20(4):5346–59.
22. Zhang K, Jiang Y, Zhao H, et al. Diverse terpenoids and their associated antifungal properties from roots of different cultivars of *Chrysanthemum morifolium* Ramat[J]. Molecules, Multidisciplinary Digital Publishing Institute. 2020;25(9):2083.
23. Wang Y, Li X, Jiang Q, et al. GC-MS analysis of the volatile constituents in the leaves of 14 Compositae plants. Molecules. 2018;23(1):166. https://doi.org/10.3390/molecules23010166
24. Bolger AM, Lohse M, Usadel B. Trimmomatic: a flexible trimmer for Illumina Sequence Data. Bioinformatics. 2014;btu170.
25. Kim D, Langmead B, Salzberg SL. HISAT: a fast spliced aligner with low memory requirements[J]. Nat Methods Nat Publishing Group. 2015;12(4):357–60.
26. Song A, Su J, Wang H, et al. Analyses of a chromosome-scale genome assembly reveal the origin and evolution of cultivated chrysanthemum[J]. Nature Communications, Nature Publishing Group. 2023;14(1):2021.
27. Yang Liao GK, Smyth W, Shi. featureCounts: an efficient general-purpose program for assigning sequence reads to genomic features[J]. Bioinf Volume. 2014;30(7):923–30.
28. Zmrzlikar J, Žganec M, Ausec L, Štajdohar M, RNAnorm. RNA-seq data normalization in Python (Version 2.0.0) [Computer software]. 2023. https://github.com/genialis/RNAnorm
29. Langfelder P, Horvath S. Fast R functions for robust correlations and hierarchical Clustering[J]. J Stat Softw. 2012;46(11):1–17.
30. Wickham H. Reshaping data with the reshape Package. J Stat Softw. 2007;21(12):1–20. http://www.jstatsoft.org/v21/i12/.
31. Wickham H. stringr: Simple, consistent wrappers for common string operations. R package version 1.5.1. 2023. https://github.com/tidyverse/stringr, https://stringr.tidyverse.org
32. Tang D, Chen M, Huang X, et al. Y.SRplot: a free online platform for data visualization and graphing. PLoS ONE. 2023;18(11):e0294236.
33. Smoot ME, Ono K, Ruscheinski J, et al. Cytoscape 2.8: new features for data integration and network visualization[J]. Bioinf (Oxford England). 2011;27(3):431–2.
34. Zheng Y, Jiao C, Sun H, et al. iTAK: a program for genome-wide prediction and classification of plant transcription factors, transcriptional regulators, and protein kinases. Molecular Plant. 2016.
35. Yu ZX, Wang LJ, Zhao B, et al. Progressive regulation of sesquiterpene biosynthesis in *Arabidopsis* and patchouli (*Pogostemon cablin*) by the miR156-targeted SPL transcription factors[J]. Molecular Plant, Elsevier. 2015;8(1):98–110.
36. Spears BJ, McInturf SA, Collins C, et al. Class I TCP transcription factor AtTCP8 modulates key brassinosteroid-responsive genes[J]. Plant Physiol. 2022;190(2):1457–73.
37. Hategan L, Godza B, Kozma-Bognar L, et al. Differential expression of the brassinosteroid receptor-encoding *BRI1* gene in *Arabidopsis*[J]. Planta. 2014;239(5):989–1001.
38. Kim Y-W, Youn J-H, Roh J, et al. Brassinosteroids enhance salicylic acid-mediated immune responses by inhibiting BIN2 phosphorylation of clade I TGA transcription factors in *Arabidopsis*[J]. Mol Plant. 2022;15(6):991–1007.
39. Liu T, Longhurst AD, Talavera-Rauh F, et al. The *Arabidopsis* transcription factor ABIG1 relays ABA signaled growth inhibition and drought induced senescence[J]. eLife. 2016;5:e13768.
40. Söderman E, Mattsson J, Engström P. The *Arabidopsis* homeobox gene *ATHB-7* is induced by water deficit and by abscisic acid[J]. Plant J. 1996;10(2):375–81.
41. Tian X, Ruan J-X, Huang J-Q, et al. Characterization of gossypol biosynthetic pathway[J]. Proc Natl Acad Sci USA. 2018;115(23):E5410–8.
42. Guo J, Zhou YJ, Hillwig ML, et al. CYP76AH1 catalyzes turnover of miltiradiene in tanshinones biosynthesis and enables heterologous production of ferruginol in yeasts[J]. Proc Natl Acad Sci USA. 2013;110(29):12108–13.
43. Teoh KH, Polichuk DR, Reed DW, et al. *Artemisia annua* L. (Asteraceae) trichome-specific cDNAs reveal CYP71AV1, a cytochrome P450 with a key role in the biosynthesis of the antimalarial sesquiterpene lactone artemisinin[J]. FEBS Lett. 2006;580(5):1411–6.
44. Haruna M, Kato M, Ito K, et al. Angeloylcumambrin-B, an antimicrobial sesquiterpene lactone from *Chrysanthemum ornatum* var. Spontaneum[J] Phytochemistry. 1981;20(11):2583–4.
45. El-Masry S, Abou-Donia AHA, Darwish FA, et al. Sesquiterpene lactones from *Chrysanthemum coronarium*[J]. Phytochemistry. 1984;23(12):2953–4.
46. Essig K, Zhao Z. Method Development and Validation of a high-performance Liquid Chromatographic Method for Pyrethrum Extract[J]. J Chromatogr Sci. 2001;39(11):473–80.
47. Cheng S-S, Wu C-L, Chang H-T, et al. Antitermitic and antifungal activities of essential oil of Calocedrus Formosana Leaf and its Composition[J]. J Chem Ecol. 2004;30(10):1957–67.
48. Storer JR, Elmore JS, Van Emden HF. Airborne volatiles from the foliage of three cultivars of autumn flowering chrysanthemums[J]. Phytochemistry. 1993;34(6):1489–92.
49. Uchio Y. Constituents of the essential oil of *Chrysanthemum japonense*. Nojigiku Alcohol and its Acetate[J]. Bull Chem Soc Jpn. 1978;51(8):2342–6.
50. Özcan MM, Chalchat JC. Chemical composition and antifungal effect of anise (*Pimpinella anisum* L.) fruit oil at ripening stage[J]. Ann Microbiol. 2006;56(4):353–8.
51. Xu Q, Zhang L, Yu S, et al. Chemical composition and biological activities of an essential oil from the aerial parts of *Artemisia Gmelinii* weber ex Stechm[J]. Volume 35. Natural Product Research, Taylor & Francis; 2021. pp. 346–9. 2.
52. Ramazani E, Akaberi M, Emami SA, et al. Pharmacological and biological effects of alpha-bisabolol: an updated review of the molecular mechanisms[J]. Life Sci. 2022;304:120728.
53. Gonzalez-Rivera ML, Barragan-Galvez JC, Gasca-Martínez D, et al. In vivo neuropharmacological effects of neophytadiene[J]. Molecules, Multidisciplinary Digital Publishing Institute. 2023;28(8):3457.
54. Hazman Ö, Bozkurt MF. Anti-inflammatory and Antioxidative Activities of Safranal in the reduction of renal dysfunction and damage that Occur in Diabetic Nephropathy[J]. Inflammation. 2015;38(4):1537–45.
55. González-Velasco HE, Pérez-Gutiérrez MS, Alonso-Castro ÁJ, et al. Anti-inflammatory and antinociceptive activities of the essential oil of *Tagetes parryi* A. Gray (Asteraceae) and verbenone[J]. Molecules, Multidisciplinary Digital Publishing Institute. 2022;27(9):2612.

56. Huang Y, Yang W, Pei Z, et al. The genes for gibberellin biosynthesis in wheat[J]. Funct Integr Genom. 2012;12(1):199–206.
57. Aharoni A, Giri AP, Deuerlein S, et al. Terpenoid metabolism in wild-type and transgenic Arabidopsis plants[J]. Plant Cell. 2003;15(12):2866–84.
58. Isemer R, Krause K, Grabe N, et al. Plastid located WHIRLY1 enhances the responsiveness of Arabidopsis seedlings toward abscisic acid[J]. Frontiers: Frontiers in Plant Science. 2012;3.

Publisher's note